Enhancement of the antitumor properties of interleukin-2 by its targeted delivery to the tumor blood vessel extracellular matrix

Barbara Carnemolla, Laura Borsi, Enrica Balza, Patrizia Castellani, Raffaella Meazza, Alexander Berndt, Silvano Ferrini, Hartwig Kosmehl, Dario Neri, and Luciano Zardi

Angiogenic processes depend on the precise coordination of different cell types and a complex exchange of signals, many of which derive from new specific components of the provisional, angiogenesis-related, extracellular matrix (ECM). Angiogenesis-associated ECM components thus represent appealing targets for the selective delivery of therapeutic molecules to newly forming tumor vessels. Results of a previous study indicated that a high affinity recombinant antibody (L19) to ED-B, a domain contained in the angiogenesis-associated isoform of fibronectin (B-FN), selectively and efficiently targets tumor vessels. The present study shows that a fusion protein between L19 and interleukin 2 (L19–IL-2) mediates the selective delivery and concentration of IL-2 to tumor vasculature, thereby leading to a dramatic enhancement of the therapeutic properties of the cytokine. By contrast, IL-2 fused to an irrelevant recombinant antibody used as a control fusion protein showed neither accumulation in tumors nor therapeutic efficacy. Tumors in mice treated with L19–IL-2 were significantly smaller compared to those in animals treated with saline, the control fusion protein, or IL-2 alone (P = .003, .003, and .002, respectively). Moreover, no significant differences in size were observed among the tumors from the different control groups (using the control fusion protein, a mixture of IL-2 and L19, or saline alone). Immunohistochemical analysis of tumor infiltrates demonstrated a significantly higher number of T lymphocytes, natural killer cells, and macrophages, as well as increased interferon-γ (IFN-γ) accumulation, in tumors from animals treated with L19–IL-2 compared to tumors from control groups. The fact that ED-B is 100% homologous in human and mouse, thus ensuring that L19 reacts equally well with human and murine antigen, should ultimately expedite transfer of this reagent to clinical trials. (Blood. 2002;99: 1659-1665)

© 2002 by The American Society of Hematology

Introduction

During tumor progression, the extracellular matrix (ECM) of the normal tissues in which the tumor grows is remodeled through 2 different processes: proteolytic degradation and neosynthesis of ECM components by both neoplastic and stromal cells. These processes generate a "tumoral ECM" that differs quantitatively and qualitatively from the normal tissue ECM and that apparently gives rise to a more suitable environment (inductive or instructive) for tumor progression.[1-3] In particular, ECM components modulate vascular cell behavior and angiogenic processes.[4,5] This observation is upheld by the recent report that the majority of messenger RNAs (mRNAs) newly expressed by tumoral endothelial cells encode for ECM proteins.[6] Thus, these provisional ECM components that appear during the angiogenic processes represent an appealing target for the selective delivery of therapeutic molecules to newly forming blood vessels.[7] Furthermore, because new vessel formation is common to all solid tumors, the angiogenesis-associated ECM components can be regarded as pan-tumoral antigens.[8-12]

One such ECM component is a fibronectin (FN) isoform, B-FN, which contains an extra FN type III repeat of 91 amino acids, the domain B (ED-B).[13] Because the amino acid sequence of ED-B is identical in mouse, humans, and other mammals, antibodies to this domain react equally well with mouse, human, and other species B-FN. B-FN is detectable only in the stroma of fetal and neoplastic tissues and around newly forming blood vessels, but not in mature vessels.[14,15] Using a radioiodinated human recombinant single-chain Fv (scFv; L19) to the ED-B domain of FN, we demonstrated in vivo the possibility of targeting newly forming tumoral blood vessels, thus laying the groundwork for the selective delivery of therapeutic agents to neovasculature.[16-20] In addition, Bircher et al[21] showed that L19, chemically coupled to a photosensitizer, selectively accumulates in the newly formed blood vessels of the rabbit cornea angiogenesis model and, after irradiation with near infrared light, mediates complete and selective occlusion of ocular neovasculature. More recently, Nilsson et al[22] reported that the immunoconjugate of L19 with the extracellular domain of tissue factor mediates selective infarction in different types of murine tumor models.

These promising findings on the targeted accumulation of therapeutic agents prompted us to investigate the efficacy in tumor

therapy of fusion proteins composed of L19 and cytokines. Interleukin 2 (IL-2) plays an essential role in the activation phases of both specific and natural immune responses.[23] Although IL-2 has no direct cytotoxic effect on cancer cells, it can induce tumor regression through its ability to stimulate a potent cell-mediated immune response in vivo.[24] However, its systemic therapeutic efficacy is limited by its rapid clearance and, at high doses, by a severe toxicity related mainly to vascular leak syndrome.[25] To overcome systemic toxicity, but, at the same time, to selectively deliver therapeutically efficacious concentrations of IL-2 to neoplastic tissues, a number of preclinical experiments on murine tumor models have been carried out using fusion proteins composed of IL-2 and antibodies with different specificities.[26-35] Although these experiments clearly proved the concept that the targeted delivery of IL-2 enhanced its therapeutic efficacy, the experiments were carried out using artificially overexpressed tumor cell surface antigens, and often the antigens were of human origin, thus making it difficult to evaluate both the accumulation in normal mouse organs and the real therapeutic efficacy of such fusion proteins.

Here we show that a fusion protein between IL-2 and L19, a human antibody that reacts equally well with a mouse and human antigen that is naturally expressed on blood vessels during angiogenic processes, mediates the selective delivery and concentration of IL-2 on tumor vasculature, thus leading to a dramatic enhancement of the therapeutic efficacy of the cytokine.

Materials and methods

Construction of L19–IL-2 and D1.3–IL-2 fusion proteins

Interleukin 2 complementary DNA (cDNA) was amplified by polymerase chain reaction (PCR) using BC-666 and BC-695 primers and, as template, the IL-2 cDNA produced by reverse transcriptase–polymerase chain reaction (RT-PCR) starting from RNA of human phytohemagglutinin (PHA)-activated peripheral blood lymphocytes.[36] The forward BC666 primer (sequence: ctcga attct cttcc tcatc gggta gtagc tcttcc ggctc atcg tccag cggcg cacct acttc aagtt ctaca) contained the *Eco*RI restriction enzyme sequence, a 45-base pair (bp) encoding for a 15 amino acid linker (SSSSG)$_3$ and 21 bases of the mature human IL-2 sequence. The reverse BC-695 primer (sequence: ctcgg atcct tatca attca gatcc tcttc tgaga tgagt ttttg ttcag tgttga gatga tgct) contained the myc tag sequence,[17] 2 stop codons, and the *Bam*HI restriction enzyme sequence. The genomic sequence of the signal secretion leader peptide was purified by digestion of the vector pUT-SEC,[37] kindly provided by Dr Oscar Burrone, Trieste, Italy, using the *Hin*dIII and *Apa*LI restriction enzymes. The human scFv L19 was amplified by PCR using the primer BC-618 (sequence: gtgtg cactc ggagg tgcag ctgtt ggagt ctggg) containing the *Apa*LI restriction enzyme and BC-679 (sequence: ctcga attct ttgat ttcca ccttg gtccc) containing the *Eco*RI restriction enzyme and the DNA vector pDNEKL19 as template. The cDNA of the scFv D1.3 was amplified using the DNA of pGIN50 described by Neri et al[18] as template, and the BC-721 (sequence: ctcgt gtgca ctcgc aggtg cagct gcagg agtca) containing the *Apa*LI restriction enzyme sequence and BC-722 (sequence: ctcga attcc cgttt gatct cgagc ttggt) containing the *Eco*RI restriction enzyme sequence as primers. Two ligations were carried out using the 3 DNA inserts (signal peptide, scFvL19 or D1.3 and IL-2) and pcDNA 3.1 mammalian expression vector (Invitrogen, Croningen, The Netherlands). The 2 clones were sequenced on both strands and expressed in P3U1 cells (American Type Culture Collection [ATCC], Rockville, MD) in the presence of G418 (750 μg/mL; Calbiochem, San Diego, CA).

Selection of clones expressing the L19–IL-2 and D1.3–IL-2 fusion proteins and their purification and characterization

The G418 resistant clones were screened for the antibody specificity of the supernatants for the ED-B or hen egg white lysozyme (Sigma, St Louis,

MO) by enzyme-linked immunosorbent assay (ELISA) as previously described by Carnemolla et al.[12] Supernatants of clones showing immunologic specificity for ED-B or lysozyme proteins were tested for IL-2 biologic activity as described by Meazza et al.[36] The L19–IL-2 and D1.3–IL-2 fusion proteins were purified from the conditioned medium of one positive clone using the recombinant ED-B fragment or the lysozyme, respectively, conjugated to Sepharose (Amersham Pharmacia Biotech, Uppsala, Sweden), by affinity chromatography as reported by Carnemolla et al.[12] The size of the 2 fusion proteins was analyzed in reducing condition on sodium dodecyl sulfate-polyacrylamide gel electrophoresis (SDS-PAGE) and in native condition by fast protein liquid chromatography gel filtration on a Superdex S-200 chromatography column (Amersham Pharmacia Biotech; data not shown).

Animals and cell lines

Athymic nude mice (8-week-old nude/nude CD1 mice, females) were obtained from Harlan Italy (Correzzana, Milan), 129 (clone S̲vHsd) strain mice (8–10-week-old mice, female) were obtained from Harlan UK (Oxon, United Kingdom). Mouse embryonal teratocarcinoma (F9), mouse T cells (CTLL-2), and mouse myeloma cells (P3U.1) were purchased from ATCC; N592, human small cell lung cancer (SCLC) cell line,[36] was kindly provided by Dr J. D. Minna (National Cancer Institute and Naval Hospital, Bethesda, MD); C51, a mouse colon adenocarcinoma cell line derived from BALB/c, was kindly provided by Dr M. P. Colombo, Milan, Italy.[38]

Biodistribution of L19–IL-2 fusion protein

Purified L19–IL-2 was radiolabeled with iodine 125 using the Iodogen method[39] (Pierce, Rockford, IL). The immunoreactive radiolabeled L19–IL-2 was more than 90%. Nude mice with subcutaneously implanted F9 murine teratocarcinoma[16] were injected intravenously with about 10 μg (4 μCi; 0.148 MBq) protein in 100 μL saline solution. Three animals were used for each time point. Mice were killed at 3, 6, and 24 hours after injection. The organs were weighed and the radioactivity was counted. All organs and tumors were placed in fixative for histologic analysis and microautoradiography. Targeting results of representative organs are expressed as percent of the injected dose per gram of tissue (%ID/g).

In vivo treatment of tumor-bearing mice with L19–IL-2 and D1.3–IL-2 fusion proteins and histologic analysis

Treatment with purified L19–IL-2 fusion protein was performed in groups of 6 mice each injected subcutaneously with 20×10^6 N592 or with 10^6 C51 or with 3×10^6 F9 cells. Twenty-four hours or 72 hours after N592, F9, and C51 cell injection, 12 μg L19–IL-2 fusion protein (corresponding to 72 000 IU) was injected into the tail vein of each animal until day 10 (Figure 3A). Similar groups of animals (6/group) were injected with a control fusion protein (D1.3–IL-2) or with a mixture of L19 (8 μg) and recombinant human IL-2 (4 μg, corresponding to 72 000 IU; proleukin, 18×10^6 UI; Chiron, Emeryville, CA) and with saline for the same number of days. At the end of treatment, animals were killed, and tumors, organs, and tissues were weighed and placed in fixative for histologic analysis. Tissue samples were cut within the largest diameter, the total and tumor areas were determined by computer aid, and the percentage of the tumor tissue was calculated.

Immunohistochemistry and image analysis

For qualitative and quantitative immunohistochemical analysis, 4-μm cryostat sections of the frozen tissue samples were fixed in ice-cold acetone for 15 minutes (the antibody PK136 was applied to native sections). The following primary antibodies were used: rat antimouse CD8a/Ly2 (clone 53-6.7); rat antimouse CD4/L3T4 (clone H129.19); rat antimouse CD11b/Mac-1α chain (clone M1/70); rat antimouse CD19 (clone 1D3); rat antimouse interferon (IFN)–γ (clone R4-6A2) (all from BD Pharmingen, San Diego, CA); rat antimouse CD31 (clone MEC 13.3) kindly supplied by A. Mantovani (Mario Negri Institute, Milan, Italy)[43]; rat antimouse CD45R/B220 (clone RA3-6B2) (Southern Biotechnology Associates, Birmingham, AL); and biotinylated mouse antimouse CD161b/c/NK1.1 (clone

PK136) (Serotec, Oxford, United Kingdom). The sections were incubated with primary antibodies overnight at 4°C. Biotinylated mouse antirat IgG2b and IgG1/2a (BD Pharmingen) were used as secondary antibodies for detection of unlabeled primary antibodies followed by the alkaline phosphatase–conjugated ABC system StreptABComplex/AP (Dako, Denmark). Naphtol-AS-biphosphate (Sigma) and new fuchsin (Merck, Darmstadt, Germany) were used as substrate and developer, respectively. To inhibit endogenous tissue enzyme activity, the developing solution was supplemented with 0.25 mM levamisole (Sigma). As negative control, the primary antibody was replaced by nonimmune serum. Sections were then counterstained with hematoxylin and mounted permanently. Quantitative analysis of inflammatory cells, IFN-γ, and microvessel density (MVD) was performed by computer-aided image analysis using the image processing and analysis system Quantimet 600 and the Qwin software (Leica, Wetzlar, Germany). A red color threshold was interactively set by the examiner for each antibody to select the red-stained immunopositive area. All pixels in the image that met the defined threshold were transferred into a binary image and analyzed. For quantitative evaluation of inflammatory cells and [IFN]-γ, in each tumor specimen the immunostained area was measured in 5 randomly selected measurement areas (total measured area 1.35 mm^2) of the tumor periphery to avoid the influence of necrosis. The results were expressed as percentage of the whole measurement area. For each animal group the mean value ± SE of all measurements was calculated.

The MVD was assessed according to Weidner at al.[40] Intratumoral MVD was evaluated by light microscopic scanning at low power of tumoral areas containing the most capillaries and small venules (so-called neovascular hot spots). The individual microvessel counts were made on a 200 × field in the neovascular hot spots, while a total tumor area of 0.3375 mm^2 was evaluated. The objects suspected by the computer-aided image analysis system as microvessels were controlled on the computer monitor before counting. The microvessel counts are given as the average of marked objects per standard area of tumor, which corresponds to one scanned counting field with a size of 0.0675 mm^2.[41] For each animal group, the mean values and SEs of all measurements were calculated.

Microautoradiography analysis and statistical analysis

Tumor and organ specimens were processed for microautoradiography to assess the pattern of ^{125}I L19–IL-2 fusion protein distribution within the tumors or organs as described by Tarli et al.[16] The statistical significance of different findings between experimental groups of animals was determined using the nonparametric Mann-Whitney test. Findings were regarded as significant if 2-tailed $P < .01$.

Results

For the preparation of scFv–IL-2 fusion proteins, we used the human scFv L19 and, for the preparation of the "control" fusion protein endowed with an irrelevant specificity, we used the scFv D1.3[42] that reacts with hen egg lysozyme but not with mouse lysozyme.

As shown in Figure 1A, the cDNA corresponding to the open reading frame of mature IL-2 was appended to the 3′ of the cDNA of the scFv by a linker of 45 bp. Chimeric cDNAs were cloned into the vector pcDNA3.1 and used to transfect mouse myeloma cells (P3U1). The 2 fusion proteins were purified from the conditioned media of the transfected cells by affinity chromatography columns. Figure 1B shows an SDS-PAGE of the 2 purified proteins. L19–IL-2 was tested for immunoreactivity of the scFv by immunohistochemistry and ELISA, and both fusion proteins were evaluated for biologic activity of IL-2 by CTLL-2 proliferation assay.[36] Equimolar amounts of IL-2 and of the fusion proteins L19–IL-2 and D1.3–IL-2 showed identical IL-2 activity. Equimolar amounts of L19–IL-2 and of scFv L19 showed identical immunoreactivity (data not shown).
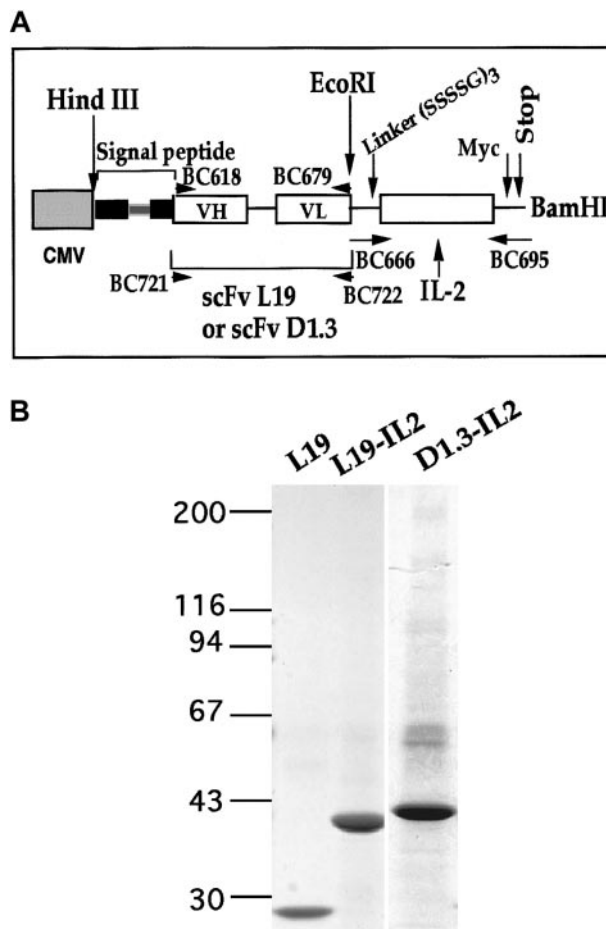

Figure 1. Preparation and characterization of fusion proteins L19–IL-2 and D1.3–IL-2. (A) Schematic representation of scFv L19–IL-2 and D1.3–IL-2 cDNA constructs. The scFv L19 or D1.3 and IL-2 cDNA were genetically fused by inserting a DNA linker (—) encoding for 15 amino acids (SSSSG)$_3$ and cloned into the pcDNA3 mammalian expression vector using the *Hind*III and *Bam*HI restriction sites.[16] The hatched box represents the CMV promoter sequence; the filled box, the genomic sequence of the signal secretion leader peptide (▬ is the intron inside the genomic sequence); and white boxes, the V$_H$ or V$_L$ of scFV L19 or D1.3 and IL-2 sequences. (B) Four percent to 18% SDS-PAGE gradient of scFv L19, L19–IL-2, and D1.3–IL-2 proteins after purification on ED-B/Sepharose affinity column. The values reported on the left indicate the molecular masses, in kilodaltons, of the standards. The fusion proteins L19–IL-2 and D1.3–IL-2 showed an apparent molecular mass of about 43 and 45 kd, respectively, in accordance with their expected sizes.

Fusion proteins were radioiodinated and intravenously injected in tumor-bearing animals for biodistribution analysis. Figure 2A shows the tumor-blood ratio of the percentage of injected dose per gram using the 2 radiolabeled proteins. Twenty-four hours after intravenous injection of radiolabeled L19–IL-2, this ratio was 33, whereas using D1.3–IL-2 it was less than 1 (Figure 2A). Using L19–IL-2, the ratio between the percentage of injected dose per gram of tumor and of the other organs, 24 hours after injection, was higher than 10. By contrast, no specific tumor accumulation was seen using the control fusion protein. Intratumoral accumulation of the radiolabeled proteins was analyzed by microautoradiography. As shown in Figure 2B, L19–IL-2 selectively accumulated around tumoral vasculature, similarly to L19 alone.[16] No accumulation was detectable using D1.3–IL-2.

To test whether the targeted delivery of IL-2 to tumor vasculature was able to inhibit tumor growth, we treated groups of syngeneic mice grafted with F9 murine teratocarcinoma with the fusion proteins L19–IL-2 or D1.3–IL-2 or saline alone. Figure 2A shows the treatment schedule used. Table 1 reports the typical
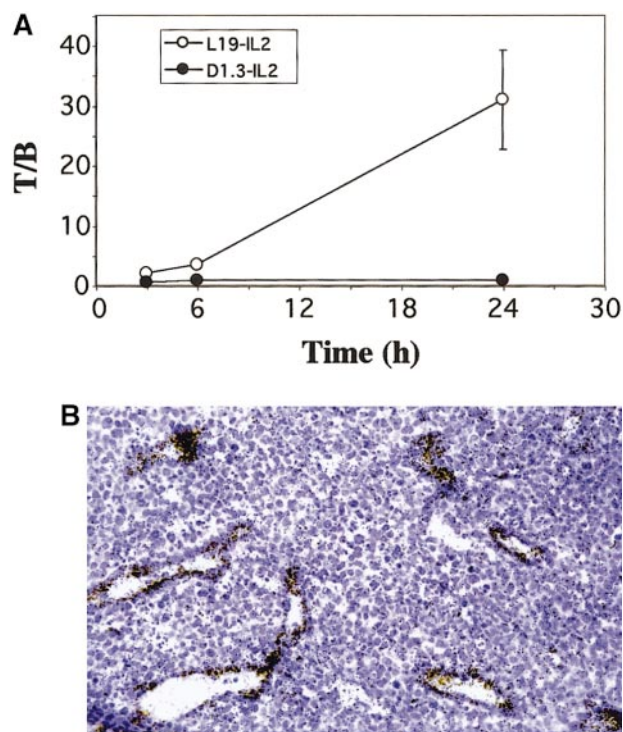
Figure 2. Biodistribution of fusion proteins L19–IL-2 and D1.3–IL-2. (A) Tumor-blood ratio (T/B) of the %ID/g at 3, 6, and 24 hours after intravenous injection of radioiodinated L19–IL-2 and D1.3–IL-2 in F9 teratocarcinoma-bearing mice. Mice with subcutaneously implanted tumors were intravenously injected with 10 μg (4 μC; 0.148 MBq) of protein in 100 μL saline solution. Three animals at each time point were killed and organs were weighed and the radioactivity counted. Vertical bars indicate SE. (B) Microautoradiography of F9 teratocarcinoma 24 hours after injection of radioiodinated L19–IL-2. Radiolabeled L19–IL-2 accumulates around tumoral vascular structures, but not around vessels of normal tissues (data not shown).

Figure 3. Treatment of tumor-bearing mice with L19–IL-2 or D1.3–IL-2 fusion proteins. (A) Upper part: treatment schedule of mice. Treatment began 72 hours after F9 murine teratocarcinoma implantation in syngeneic mice; mice received daily intravenous injections of 12 μg L19–IL-2 or D1.3–IL-2 corresponding to 72 000 IU, or saline for 6 consecutive days. Animals were killed on the 10th day. The photograph shows the F9 tumors dissected from the different groups of animals. (B) Immunohistochemistry using a rat antimouse CD 45R/B220 antibody of the F9 tumor from a mouse treated with D1.3–IL-2 (i) and from a mouse treated with L19-IL-2 (ii). Scale bar indicates 30 μm.

results obtained treating tumor-bearing mice for 6 days with daily intravenous doses of 72 000 U IL-2 per mouse as either L19–IL-2 or D1.3–IL-2. Figure 3A shows the tumors removed from the 3 groups of mice at the end of the treatment. The weights of tumors from animals treated with L19–IL-2 were compared to those from animals treated with D1.3–IL-2 using the Mann-Whitney statistical test and were found to be highly significantly different ($P = .003$, Table 1).

Table 1. Histologic analysis of F9 tumor growth in syngeneic mice treated with L19–IL-2 and D1.3–IL-2 fusion proteins

	Treatment		
	L19–IL2	D1.3–IL2	Saline
Weight of tumors (g)	0.05 ± 0.01	0.597 ± 0.1	0.811 ± 0.23
TILs*	53.2 ± 13.8	0.75 ± 0.14	0.52 ± 0.26
M/HPF	5.2 ± 1.5	13.8 ± 1.6	12.4 ± 2.7
% of connective tissue and necrosis area with respect to total tumor area	77.3	18.5	11.1

The nonparametric Mann-Whitney test was used to determine the statistical significance of differences in tumor weights among the three groups of animals. The differences in tumor weights following treatment with the fusion protein L19–IL-2 were statistically significant compared to treatment with phosphate-buffered saline (PBS) or D1.3–IL-2 fusion protein (L19–IL-2/D1.3–IL-2, $P = .003$; L19–IL-2/PBS, $P = .003$; D1.3–IL-2/PBS: $P = .423$).

TIL indicates tumor-infiltrating lymphocytes; M/HPF, mitoses per high-power field.

*The quantitative evaluation of CD45R/B220$^+$ cells was carried out using a rat antimouse CD45/B220 in immunohistochemistry. Values reported represent the mean number of positive TIL/HPF ± SE.

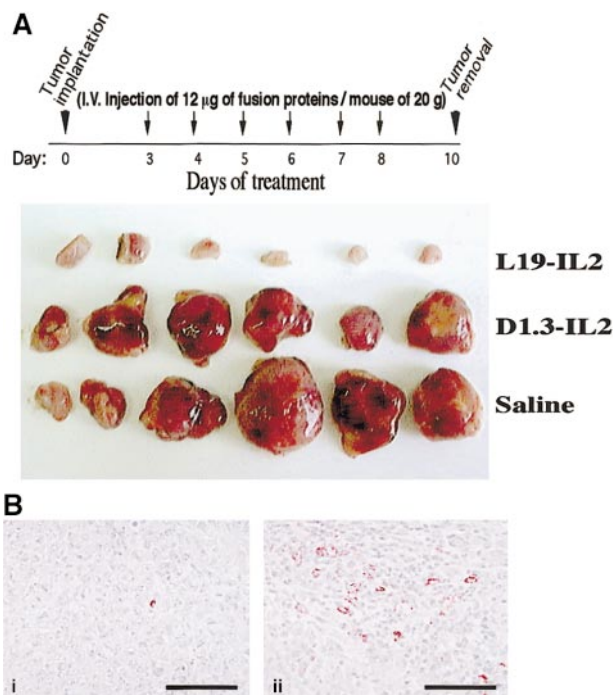Tumors were also analyzed histologically and immunohistochemically, and the results are summarized in Table 1. The major observations were: (1) a higher lymphocyte infiltration in tumors from animals treated with L19–IL-2 with respect to controls (about 70 times higher with respect to animals treated with D1.3–IL-2 and 100 times higher with respect to animals treated with saline as shown in Figure 3B); (2) the amount of connective tissue and necrosis in tumors from animals treated with L19–IL-2 was nearly 70% of the tumor mass, but only 18% and 11% in tumors from animals treated with D1.3–IL-2 and saline, respectively. Similar results were obtained using different tumor models such as C51 murine adenocarcinoma and N592 human SCLC (Table 2). No

Table 2. Effect on tumor growth of L19–IL-2 fusion protein

Tumor cell lines	L19–IL-2 fusion protein	IL–2/L19*	Saline	D1.3–IL-2 fusion protein
C51†	0.017 ± 0.008‡	0.228 ± 0.06	0.410 ± 0.07	0.251 ± 0.07
N592†	0.173 ± 0.07	0.705 ± 0.13	1.178 ± 0.3	ND
N592†	0.075 ± 0.02	ND	0.608 ± 0.08	0.385 ± 0.1
F9†	0.061 ± 0.06§	0.665 ± 0.28	1.715 ± 0.23	ND
F9‖	0.05 ± 0.012	ND	0.811 ± 0.24	0.597 ± 0.1
F9‖	0.088 ± 0.04	ND	1.3 ± 0.36	0.9 ± 0.43

Values reported represent the mean tumor weight (g) ± SE; groups of 6 mice were used for each experiment.

ND indicates not determined.

*Equimolar mixture of scFv L19 and recombinant IL-2.

†Tumoral cells grown in athymic nude mice.

‡A tumoral mass grew in only 4 of 6 mice.

§A tumoral mass grew in only 3 of 6 mice.
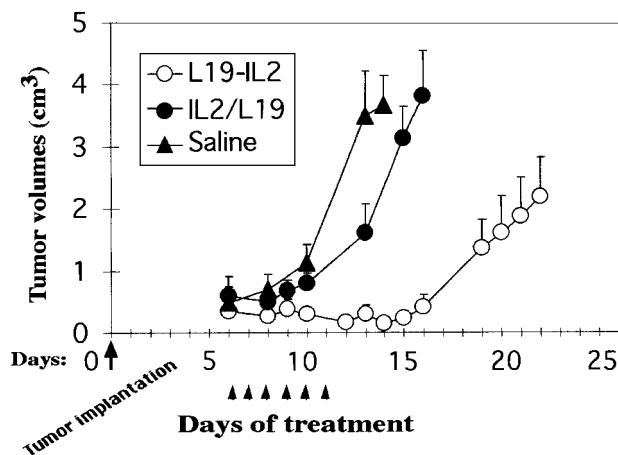
‖Tumoral cells grown in syngeneic 129 strain mice.

Figure 4. Growth inhibition of established tumors with L19–IL-2 fusion protein. Volumes (cm³) of F9 teratocarcinoma tumors from syngeneic mice after 6 days of intravenous treatment with 250 000 IU of IL-2 as L19–IL-2 or as an equimolar mixture of IL-2 and L19 or with saline. Each group comprised 6 mice. Therapy was started 6 days after tumor implantation, when tumor size was 0.4 to 0.5 cm³. Arrowheads indicate the days of treatment. Tumor size was determined by caliper measurements in 2 perpendicular dimensions, and tumor volume was determined according to the formula: (short dimension)^2 × (long dimension) × 0.52.[16] SEs are indicated.

significant differences were observed in tumors grafted in syngeneic or athymic nude mice, suggesting that the antitumor response may occur in the absence of T cells.

We also tested the ability of L19–IL-2 to inhibit the growth of well-established tumors. Six days after grafting F9 teratocarcinoma into syngeneic mice, tumors reached a volume of nearly 0.4 to 0.5 cm³. Three groups of these animals were then treated for 6 days with daily intravenous injection of 250 000 U IL-2 as L19–IL-2, unconjugated IL-2/L19 mixture, or saline alone. The results, depicted in Figure 4, show that although L19–IL-2 induced a regression of about 50% of the tumor mass, the mixture of unconjugated IL-2/L19 did not significantly inhibit tumor growth compared to treatment with saline alone. In the group of animals treated with L19–IL-2, the tumor masses remained stable until 5 days after interruption of treatment; thereafter, tumors resumed growth, but at a reduced rate compared to controls (Figure 4).

Using a panel of antibodies, we studied and compared the inflammatory cells infiltrating the tumors from the groups of animals treated with the fusion protein L19–IL-2, an equimolar mixture of IL-2 and L19, or saline. We also studied the amount of IFN-γ, as well as the MVD, in tumors. Immunohistochemical analysis of tumor samples revealed an enhanced accumulation of CD8$^+$ cytotoxic T lymphocytes, as well as an increase of CD4$^+$ cells in the tumors of animals treated with L19–IL-2 compared to tumors from control group mice. An increased accumulation of CD11b$^+$ cells (macrophages and natural killer [NK] cells), as well as NK1.1$^+$ cells (NK cells), was also seen in the tumors of animals treated with L19–IL-2. A significantly enhanced accumulation of

IFN-γ was observed in the tumors of animals treated with L19–IL-2 compared to tumors from the control groups of animals, whereas no B-lymphocyte (CD19$^+$ cells) infiltration was seen in tumors from any group of treated animals (Table 3).

We also studied immunohistochemically the MVD in non-necrotic, nonfibrotic areas of tumor sections from different groups of animals using a monoclonal antibody specific for mouse CD31.[43] We observed only a slight reduction of MVD in the tumor tissues of mice treated with L19–IL-2 compared to the tumors from animals of the control groups (Table 3).

Discussion

The targeted delivery of cytokines to solid tumors using antibody-cytokine fusion proteins represents a promising strategy in cancer immunotherapy. This approach achieves the purpose of selectively distributing cytokine concentrations sufficient to elicit a significant antitumor activity in primary and disseminated tumors, while limiting systemic toxicity.

We chose to selectively deliver therapeutic agents to tumor ECM components, which are generally more abundant and stable with respect to tumor-associated cell surface antigens.[7] Here we report the preclinical therapeutic evaluation of the fusion protein L19–IL-2, which binds to the provisional tumor ECM component B-FN, a marker of angiogenesis. We show that L19–IL-2, injected intravenously in tumor-bearing mice, accumulates selectively around tumor blood vessels, as does the scFv L19 alone.[16]

Using murine tumor models, we found that L19–IL-2 inhibits tumor growth more effectively than either the control fusion protein D1.3–IL-2 or an equimolar mixture of IL-2 and L19. In all 3 experimental animal models we studied, most of the tumor mass (70%) in animals treated with L19–IL-2 was composed of connective and necrotic tissue. In addition, a dramatic increase in lymphocyte infiltration and IFN-γ was observed in tumors from animals treated with the L19–IL-2 fusion protein compared to tumors from control groups of animals. The increased expression of IFN-γ and the massive infiltration of cytotoxic T lymphocytes, macrophages, and NK cells in the tumor environment could explain the therapeutic effects observed. Furthermore, IFN-γ has been demonstrated to directly inhibit the growth of a number of tumor cell lines. In addition, IFN-γ has been shown to act as a secondary mediator of the antitumor activity of several cytokines such as IL-2, IL-12, and IL-15.[44] The observed increased level of NK cells could also explain the anticancer activity of the L19–IL-2 fusion protein seen in athymic mice.

Moreover, because endothelial cells migrate along the fibers of the provisional ECM, and because IL-2 is known to be cytotoxic to endothelial cells,[25] the possibility to selectively deposit IL-2, and thereby convey cytotoxic properties to this ECM, should allow the cytokine to more effectively elicit its cytotoxic action on migrating

Table 3. Tumor-infiltrating inflammatory cells and tumor MVD

Treatment	CD19	CD4	CD8	CD11b	NK1.1	IFN–γ	MVD
Saline	0	0.37 ± 0.17	0.55 ± 0.27	11.56 ± 2.55	10.63 ± 9.01	8.10 ± 2.19	39.65 ± 3.52
IL-2/L19 mix	0	0.74 ± 0.24	0.60 ± 0.35	18.92 ± 4.19	5.58 ± 2.86	4.29 ± 1.51	38.1 ± 1.90
L19–IL-2	0	2.13 ± 0.50	9.75 ± 6.45	38.16 ± 7.42	26.42 ± 6.38	29.34 ± 8.04	33.83 ± 2.97

A mouse colon adenocarcinoma cell line (C51) was subcutaneously implanted in syngeneic mice. Three days after implantation, animals were treated with L19–IL-2 fusion protein or IL-2/L19 mix (72 000 IU IL-2) or saline by daily injection into the tail vein for 6 days. Tumor sections from the 3 different groups were immunohistochemically analyzed with a panel of antibodies. Values represent stained area as % of the measurement frame area (500 × 370 μm), ± SE (see "Materials and methods"). The differences in the levels of CD8, NK, and IFN-γ among tumors from animals treated with the fusion protein L19–IL-2 and an equimolar mixture of IL-2/L19 were statistically highly significant ($P <$ .02). On the contrary, no statistically significant differences were observed in any of the tested antigens in tumors from animals treated with the mixture IL-2/L19 or saline alone.

endothelial cells. To assess this possibility, we measured the MVD in neovascular of tumors, and found only a slight decrease in tumoral MVD in animals treated with L19–IL-2 compared to animals receiving a mixture of IL-2 and L19 or saline alone. Nevertheless, considering that necrotic and fibrotic areas represented more than 70% of the total mass of the tumors from animals treated with L19–IL-2, we cannot rule out a priori that the direct cytotoxic effect of IL-2 on endothelial cells could have contributed to the generation of the observed fibrosis and necrosis. Further experiments are needed to validate or disprove this concept.

Furthermore, the targeted delivery of therapeutic agents to the subendothelial ECM could also help to overcome one of the major problems hindering cancer therapy, namely, the poor delivery of drugs owing to the interstitial hypertension that is characteristic of solid tumors.[45,46] The L19–IL-2 fusion protein reported here serves this purpose, because it binds avidly to B-FN, which is a component of the subendothelial matrix of blood vessels during angiogenic processes. We have set up an assay to quantitatively determine B-FN in tissues from murine experimental tumor models and from fragments of human tumors. Our results indicate that in the murine teratocarcinoma F9 there are about 300 μg B-FN/g fresh tissue. This figure is similar to the levels of B-FN found in human tumors; in fact, we found from 125 to 320 μg B-FN/g fresh tissue in different specimens of human lung cancer, and from 100 to 400 μg B-FN/g in specimens of human glioblastoma, whereas in normal lung and brain tissues B-FN was undetectable (L.Z., unpublished results, manuscript in preparation).

In conclusion, we demonstrate that the targeted delivery of IL-2 to provisional, angiogenesis-related ECM components is feasible and therapeutically effective. Furthermore, because B-FN is a naturally occurring angiogenesis marker identical in mouse and in humans, and because the amount of ED-B in human tumors is similar to that expressed in murine tumor models, the scFv L19 appears to be a very powerful and fitting reagent to be used as a means to deliver a variety of effector molecules to newly forming blood vessels, thus providing a new approach to therapy for solid tumors.

Acknowledgment

References

1. Folkman J. Angiogenesis in cancer, vascular, rheumatoid and other diseases. Nat Med. 1995;1: 27-31.

2. Risau W, Lemmon V. Changes in the vascular extracellular matrix during embryonic vasculogenesis and angiogenesis. Dev Biol. 1988;125: 441-450.

3. Van Den Hoff A. Stromal involvement in malignant growth. Adv Cancer Res. 1988;50:159-196.

4. Madri J-A. Extracellular matrix modulation of vascular cell behavior. Transplant Immunol. 1997;5: 179-183.

5. Folkman J, D'Amore P-A. Blood vessel formation: what is its molecular basis? Cell. 1996;87:1153-1155.

6. St Croix B, Rago C, Velculescu V, et al. Genes expressed in human tumor endothelium. Science. 2000;289:1197-1202.

7. Neri D, Zardi L. Affinity reagents against tumour-associated extracellular molecules and new forming vessels. Adv Drug Deliv Rev. 1998;31:43-52.

8. Arap W, Pasqualini R, Ruoslahti E. Chemotherapy targeted to vasculature. Curr Opin Oncol. 1998;10:560-565.

9. Arap W, Pasqualini R, Ruoslahti E. Cancer treatment by targeted drug delivery to tumor vasculature in a mouse model. Science. 1998;279:377-380.

10. Pasqualini R, Koivunen E, Ruoslahti E. α v integrins as receptors for tumor targeting by circulating ligands. Nat Biotechnol. 1997;15:542-546.

11. Pasqualini R, Koivunen E, Kain R, et al. Aminopeptidase N is a receptor for tumor-homing peptides and a target for inhibiting angiogenesis. Cancer Res. 2000;60:722-727.

12. Carnemolla B, Neri D, Castellani P, et al. Phage antibodies with pan-species recognition of the oncofoetal angiogenesis marker fibronectin ED-B domain. Int J Cancer. 1996;68:397-405.

13. Zardi L, Carnemolla B, Siri A, et al. Transformed human cells produce a new fibronectin isoform by preferential alternative splicing of a previously unobserved exon. EMBO J. 1987;6:2337-2342.

14. Carnemolla B, Balza E, Siri A, et al. A tumor-associated fibronectin isoform generated by alternative splicing of messenger RNA precursors. J Cell Biol. 1989;108:1139-1148.

15. Castellani P, Viale G, Dorcaratto A, et al. The fibronectin isoform containing the ED-B oncofetal domain: a marker of angiogenesis. Int J Cancer. 1994;59:612-618.

16. Tarli L, Balza E, Viti F, et al. A high-affinity human antibody that targets tumoral blood vessels. Blood. 1999;94:192-198.

17. Viti F, Tarli L, Giovannoni L, Zardi L, Neri D. Increased binding affinity and valence of recombinant antibody fragments lead to improved targeting of tumoral angiogenesis. Cancer Res. 1999; 59:347-353.

18. Neri D, Carnemolla B, Nissim A, et al. Targeting by affinity-matured recombinant antibody fragments of an angiogenesis associated fibronectin isoform. Nat Biotechnol. 1997;15:1271-1275.

19. Demartis S, Tarli L, Borsi L, Zardi L, Neri D. Selective targeting of tumour neo-vasculature by a radiohalogenated human antibody fragment specific for the ED-B domain of fibronectin. Eur J Nucl Med. 2001;28:534-539.

20. Pini A, Viti F, Santucci A, et al. Design and use of a phage display library. Human antibodies with subnanomolar affinity against a marker of angiogenesis eluted from a two-dimensional gel. J Biol Chem. 1998;273: 21769-21776.

21. Bircher M-B, Viti F, Zardi L, Spiess B, Neri D. Selective targeting and photocoagulation of ocular angiogenesis mediated by a phage-derived human antibody fragment. Nat Biotechnol. 1999;17: 984-988.

22. Nilsson F, Kosmehl H, Zardi L, Neri D. Targeted delivery of tissue factor to the ED-B domain of fibronectin, a marker of angiogenesis, mediates the infraction of solid tumors in mice. Cancer Res. 2001;61:711-716.

23. Taniguchi T, Minami Y. The IL-2/IL-2 receptor system: a current overview. Cell. 1993;73:5-8.

24. Rosenberg S-A. Interleukin-2 and the development of immunotherapy for the treatment of patients with cancer. Cancer J Sci Am. 2000;6:2-7.

25. Baluna R, Rizo J, Gordon B-E, Ghetie V, Vitetta E-S. Evidence for a structural motif in toxins and interleukin-2 that may be responsible for binding to endothelial cells and initiating vascular leak syndrome. Proc Natl Acad Sci U S A. 1999;96: 3957-3962.

26. Fell H-P, Gayle M-A, Grosmaire L, Ledbetter J-A. Genetic construction and characterization of a fusion protein consisting of a chimeric F(ab′) with specificity for carcinomas and human IL-2. J Immunol. 1991;146:2446-2452.

27. Savage P, So A, Spooner R-A, Epenetos A-A. A recombinant single chain antibody interleukin-2 fusion protein. Br J Cancer. 1993;67:304-310.

28. Sabzevari H, Gillies S-D, Mueller B-M, Pancook J-D, Reisfeld R-A. A recombinant antibody-interleukin 2 fusion protein suppresses growth of hepatic human neuroblastoma metastases in severe combined immunodeficiency mice. Proc Natl Acad Sci U S A. 1994;91:9626-9630.

29. Becker J-C, Pancook J-D, Gillies S-D, Furukawa K, Reisfeld R-A. T cell-mediated eradication of murine metastatic melanoma induced by targeted interleukin 2 therapy. J Exp Med. 1996;183:2361-2366.

30. Harvill E-T, Fleming J-M, Morrison S-L. In vivo properties of an IgG3–IL-2 fusion protein. A general strategy for immune potentiation. J Immunol. 1996;157:3165-3170.

31. Melani C, Figini M, Nicosia D, et al. Targeting of interleukin 2 to human ovarian carcinoma by fusion with a single-chain Fv of antifolate receptor antibody. Cancer Res. 1998;58:4146-4154.

32. Lode H-N, Xiang R, Dreier T, Varki N-M, Gillies S-D, Reisfeld R-A. Natural killer cell-mediated eradication of neuroblastoma metastases to bone marrow by targeted interleukin-2 therapy. Blood. 1998;91:1706-1715.

33. Xu X, Clarke P, Szalai G, et al. Targeting and therapy of carcinoembryonic antigen-expressing tumors in transgenic mice with an antibody-interleukin 2 fusion protein. Cancer Res. 2000;60: 4475-4484.

34. Lode H-N, Reisfeld R-A. Targeted cytokines for cancer immunotherapy. Immunol Res. 2000;21: 279-288.

35. Penichet M-L, Morrison S-L. Antibody-cytokine fusion proteins for the therapy of cancer. J Immunol Methods. 2001;248:91-101.

36. Meazza R, Marciano S, Sforzini S, et al. Analysis of IL-2 receptor expression and of the biological effects of IL-2 gene transfection in small-cell lung cancer. Br J Cancer. 1996;74:788-795.

37. Li E, Pedraza A, Bestagno M, Mancardi S, Sanchez R, Burrone O. Mammalian cell expression of dimeric small immune proteins (SIP). Protein Eng. 1997;10:731-736.

38. Colombo M-P, Forni G. Immunotherapy I. Cytokine gene transfer strategies. Cancer Metastasis Rev. 1997;16:421-432.

39. Riske F, Hakimi J, Mallamaci M, et al. High affinity human IgE receptor (Fc epsilon RI); analysis of functional domains of the alpha-subunit with monoclonal antibodies. J Biol Chem. 1991; 266: 11245-11251.

40. Weidner N, Semple JP, Welch WR, Folkmann J. Tumour angiogenesis and metastasis-correlation in invasive breast carcinoma. N Engl J Med. 1991;324:1-7.

41. Herbst C, Kosmehl H, Stiller K-J, et al. Evaluation of microvessel density by computerised image

analysis in human renal cell carcinoma. Correlation to tumor size, nuclear grade, proliferative activity and occurrence of metastasis. J Cancer Res Clin Oncol. 1998;124:141-147.

42. McCafferty J, Griffiths A-D, Winter G, Chiswell D-J. Phage antibodies: filamentous phage displaying antibody variable domains. Nature. 1990; 348:552-554.

43. Vecchi A, Garlanda C, Lampugnani MG, et al. Monoclonal antibodies specific for endothelial cells of mouse blood vessels. The identification of adult and embryonic endothelium. Eur J Cell Biol. 1994;63:247-254.

44. Tannenbaum CS, Hamilton TA. Immune-inflam-

matory mechanisms in IFN gamma-mediated anti-tumor activity. Semin Cancer Biol. 2000;10: 113-123.

45. Jain R-K, Baxter L-T. Mechanisms of heterogeneous distribution of monoclonal antibodies and other macromolecules in tumors: significance of elevated interstitial pressure. Cancer Res. 1988; 48:7022-7032.

46. Jain R-K. Vascular and interstitial physiology of tumors: role in cancer detection and treatment. In Bicknell R, Lewis CE, Ferrara N, eds. Tumour Angiogenesis. New York, NY: Oxford University Press; 1997:45-59.